

The melting curve of neon at high pressure

Cite as: J. Chem. Phys. **94**, 3835 (1991); <https://doi.org/10.1063/1.460683>

Submitted: 18 October 1990 . Accepted: 19 November 1990 . Published Online: 31 August 1998

W. L. Vos, J. A. Schouten, D. A. Young, and M. Ross



View Online



Export Citation

ARTICLES YOU MAY BE INTERESTED IN

[Structure and compression of crystalline argon and neon at high pressure and room temperature](#)

Applied Physics Letters **39**, 892 (1981); <https://doi.org/10.1063/1.92597>

[BX90: A new diamond anvil cell design for X-ray diffraction and optical measurements](#)

Review of Scientific Instruments **83**, 125102 (2012); <https://doi.org/10.1063/1.4768541>

[Specific volume measurements of Cu, Mo, Pd, and Ag and calibration of the ruby R₁ fluorescence pressure gauge from 0.06 to 1 Mbar](#)

Journal of Applied Physics **49**, 3276 (1978); <https://doi.org/10.1063/1.325277>

The Journal
of Chemical Physics

Submit Today

The Emerging Investigators Special Collection and Awards
Recognizing the excellent work of early career researchers!



The melting curve of neon at high pressure

W. L. Vos and J. A. Schouten

van der Waals Laboratorium, Universiteit van Amsterdam, Valckenierstraat 67, 1018 XE Amsterdam, The Netherlands

D. A. Young and M. Ross

Lawrence Livermore National Laboratory, University of California, Livermore, California 94550

(Received 18 October 1990; accepted 19 November 1990)

We have measured the melting curve of neon to 54.5 kbar and 328 K using a diamond-anvil cell. The measured points together with earlier low-pressure data are fitted accurately with a Simon-Glatzel function. Theoretical calculations of the melting curve using lattice dynamics and variational fluid theory with exponential-six potentials fitted to solid isotherm data are in good agreement with the experimental data. The law of corresponding states is tested for the melting curves of He, Ne, and Ar, and is found to be obeyed.

I. INTRODUCTION

Melting is a phenomenon that is still under intensive investigation.¹⁻³ Although the thermodynamic basis of phase equilibrium is well understood, the accurate prediction of melting curves provides a severe test for statistical-mechanical theories and our knowledge of intermolecular potentials. Recent advances in the diamond-anvil cell method have extended accurate measurements of isotherms and melting curves to higher pressures and have given a new impetus to the study of melting.

Previous theoretical studies have shown that the intermolecular potentials which are obtained by fitting solid isotherm data can be used with theoretical models to correctly predict melting curves.³⁻⁵ The interaction of rare-gas atoms at high density is well described by an exponential-six potential with a stiffness parameter $\alpha = 13.0-13.2$. As a consequence, all of the properties of these elements may be scaled to universal functions and the melting curves can be placed on a reduced plot, with the exception of helium over the range in which quantum effects are significant.

Thus from the point of view of melting, the most interesting elements are the rare gases and of these the most important are helium and neon, which can achieve the highest reduced temperatures and pressures. In a recent paper, Vos *et al.*⁶ reported measurements of the melting curve of helium up to 240 kbar and 460 K. The p - T melting curve of neon has been measured by Crawford and Daniels⁷ up to 10 kbar and a single point at room temperature was obtained by Finger *et al.*⁸ The melting curve of argon has been measured to 60 kbar and 717 K.⁵

In this paper we present new measurements of the melting curve for neon up to 54.5 kbar and 328 K. These measurements are in good agreement with theoretical calculations using intermolecular potentials fitted to the various solid and fluid isotherm data. We also show that the elements He, Ne, and Ar obey a corresponding states scaling of their melting curves over the classical regime.

II. EXPERIMENTAL METHOD AND RESULTS

The experiments were performed in a diamond-anvil cell (DAC) described previously.⁹ The well-known ruby

pressure scale is used with a pressure coefficient taken as 0.0366 nm/kbar.¹⁰ Heating was accomplished through an electrical coil wound on a cold finger that is connected to a copper ring surrounding the cell.

Two sets of experiments were performed with gaskets made of K monel. The temperature dependence of the ruby lines was measured at ambient pressure before and after each set of experiments and the average was taken. The ruby was illuminated with an argon-ion laser (SP-162) at beam powers below 10 mW to prevent heating. We estimate the error in the absolute value of the pressure to be about 0.4 kbar, but the relative error is much smaller. The gas used was of research grade with a purity better than 99.998%.

The sample space was loaded by mounting the DAC in a high-pressure vessel and pressurizing it with neon. The cell was closed at a pressure of a few kbar and placed in the main frame for further pressurizing the sample. The temperature was measured with a calibrated platinum resistance thermometer. We estimate the accuracy of the temperature measurement to be better than 0.5 K. The temperature range was limited because at the time of the experiment, the DAC setup was not suitable for temperatures above 330 K.

The detection method used is quasi-isochoric scanning.¹¹ In this method, the temperature of the DAC is varied in steps of about 1 K and the pressure is measured at every temperature. We waited 15 min for temperature equilibrium. In order to check that the equilibrium was obtained, some runs were performed with increasing as well as decreasing temperature. No difference was observed. Although we were able to observe the phase equilibrium visually, it was difficult, since there was hardly any difference in the refractive index of the solid and fluid phases. They could only be distinguished due to the presence of an interface. Therefore, all data points were taken with the quasi-isochoric scanning method. An example of such a scan is shown in Fig. 1. At low temperature, the pressure is nearly constant in the solid phase. Then, the pressure increases due to melting and, finally, it is again nearly constant in the fluid phase. The small jump at 283 K is caused by a slight undercooling, since this scan was taken with decreasing temperature. The undercooling was always small (< 5 K), in contrast to our experience with other substances.

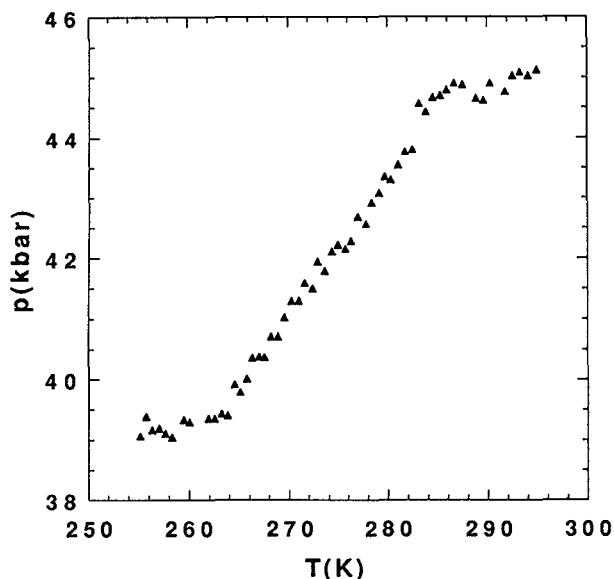


FIG. 1. A quasi-isochoric p - T scan across the melting curve of neon.

Since many data points were obtained, we have listed only the midpoints of the transition in Table I for clarity. The midpoints are plotted in Fig. 2. It can be seen that they are a smooth continuation of the data of Crawford and Daniels.⁷ The datum of Finger, *et al.*⁸ at 293 K lies about 0.8 kbar higher than our data, which is within the combined error bars of both experiments ($0.5 + 0.4$ kbar). Our data lie close to the extrapolation of the modified Simon-Glatzel (SG) equation of Crawford and Daniels⁷

$$p(\text{kbar}) = 0.015\,707\,74 \times [T(\text{K}) - 11.685]^{1.418\,52} - 0.587\,70. \quad (1)$$

It was not possible to fit a normal SG equation to all data including those of Crawford and Daniels within experimental accuracy. This can also be appreciated from the fact that an extrapolation of the unmodified SG equation fitted by these authors deviates about 2 kbar at our highest experimental point. Therefore, we followed the suggestion of

TABLE I. The melting curve of neon.

$T(\text{K})$	$p(\text{kbar})$
143.3	15.7
177.4	21.8
197.7	25.9
270.6	41.3
273.5	41.8
288.4	45.4
293.5	46.4
294.2	46.6
321.3	52.8
327.9	54.5

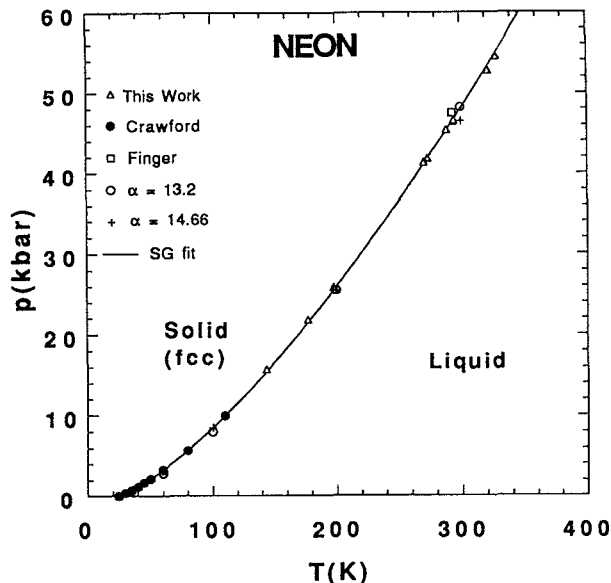


FIG. 2. The melting curve of neon. The earlier experimental data are shown together with this work. The Simon-Glatzel fit of Eq. (2) is shown as a smooth curve. The theoretical predictions from the $\alpha = 13.2$ and $\alpha = 14.66$ exp-6 potentials are shown as points.

Crawford and Daniels that a normal SG equation fits well at reduced pressures $p^* = p\sigma^3/\epsilon$ larger than 15, where σ is the distance of the zero crossing of the potential. With neon, this corresponds to a pressure of about 3 kbar. Indeed, an unmodified SG equation can be fitted to all data points at pressures above 3 kbar, yielding

$$p(\text{kbar}) = 0.012\,062 \times T(\text{K})^{1.4587} - 1.478 \quad (2)$$

with a standard deviation of 0.3 kbar. This curve is shown in Fig. 2. However, it should be observed that at high temperatures, a modified SG equation reduces to a normal SG equation, since T becomes much larger than the accompanying constant term.

III. THEORETICAL

The theoretical calculation of the melting curve of neon was performed by the same method previously used in the study of hydrogen³, helium⁴, and argon.⁵ Here the solid free energy is computed as the sum of the quasiharmonic lattice dynamics and classical plus quantum anharmonic contributions, and the liquid free energy is computed from the soft-sphere variational theory with a Wigner-Kirkwood quantum correction. The intermolecular potential used in the calculations is an exponential-six potential

$$\phi(r) = \epsilon \left\{ \frac{6}{\alpha - 6} \exp \left[\alpha \left(1 - \frac{r}{r_m} \right) \right] - \frac{\alpha}{\alpha - 6} \left(\frac{r_m}{r} \right)^6 \right\}, \quad (3)$$

where ϵ is the well depth, r_m is the position of the potential minimum, and α is the stiffness parameter. The three adjustable parameters ϵ , r_m , α are fitted to the available experimental isotherms.^{8,12-14} There are data from three experi-

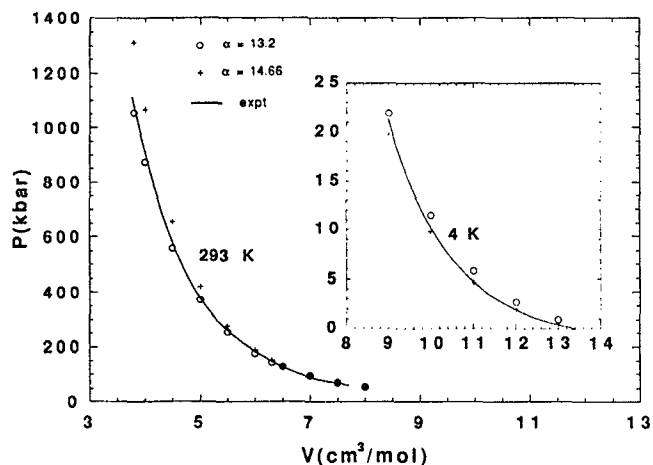


FIG. 3. A comparison of experimental solid neon isotherms with theoretical predictions. The inset shows the low-pressure region. The units are the same in the main graph and in the inset.

mental solid Ne isotherms: (1) piston cylinder at 4 K to 20 kbar;¹² (2) DAC at 293 K to 150 kbar;⁸ and (3) DAC at room temperature (293 K) to 1.1 Mbar.¹³ In addition, there is one fluid isotherm at 298 K to 10 kbar obtained by an expansion technique.¹⁴ The experimental isotherms are compared with theoretical calculations in Figs. 3 and 4.

The best overall fit was obtained with $\epsilon/k = 42.0$ K, $r_m = 3.18$ Å, and $\alpha = 13.2$, which is shown in Fig. 3. As can be seen, the fit predicts pressures which are too high for the low-pressure range and slightly too low for the high-pressure range. An accurate fit to low-pressure fluid p - V and sound-

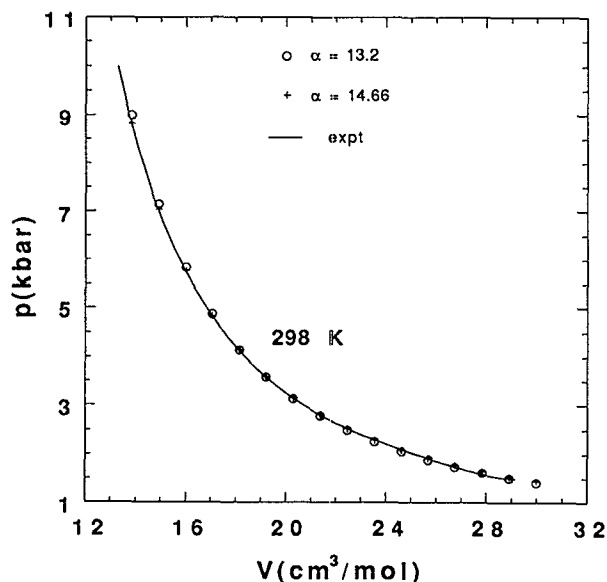


FIG. 4. A comparison of experimental liquid neon isotherm with theoretical predictions.

speed data was given by Kortbeek and Schouten¹⁵ with $\epsilon/k = 36.486$ K, $r_m = 3.121$ Å, and $\alpha = 14.660$. This potential gives a better fit to low-pressure Ne thermodynamic data and remains good even up to 250 kbar in the solid state, but deviates, as expected for a large value of α , from the highest-pressure isothermal data.

The melting curves calculated using both potentials are compared with experimental data in Fig. 2. It is seen that the Kortbeek ($\alpha = 14.66$) potential gives a better fit to experiment at low pressures, but that the overall fit ($\alpha = 13.2$) is better at the higher melting pressures. It is clear from this that the accuracy of the predicted melting curves reflects the accuracy of the potential fits to the isothermal data. The solidus volume V_s has been measured up to 53.5 K and the liquidus volume V_l up to 33 K for Ne.¹⁶ The $\alpha = 14.660$ potential is clearly better at low pressures. At the triple point ($T = 24.55$ K), the experimentally determined liquid and solid volumes¹⁶ are 16.18 and 14.17 cm³/mol, while the $\alpha = 14.660$ potential yields 16.40 and 13.90 cm³/mol and the $\alpha = 13.2$ potential 17.71 and 14.77 cm³/mol. The predictions using the two potentials converge near 200 K. The theoretical melting results for the two calculations are listed in Tables II and III.

The availability of high-pressure isotherms and melting data for He, Ne, and Ar provide an opportunity for testing the theory of corresponding states. The melting curves of these elements have now been calculated with exp-6 potentials with α varying between 13.0 and 13.2. The constancy of the stiffness parameter α indicates that the properties of the three elements "correspond." This can be checked by scaling the He and Ar data by ratios to bring them onto the Ne temperature and pressure scales. For example, the Ar melting pressures and temperatures may be scaled to those of Ne by the expressions

$$p(\text{Ar} \rightarrow \text{Ne}) = p(\text{Ar}) \times \frac{\epsilon/r_m^3(\text{Ne})}{\epsilon/r_m^3(\text{Ar})} \quad (4)$$

and

$$T(\text{Ar} \rightarrow \text{Ne}) = T(\text{Ar}) \times \frac{\epsilon/k(\text{Ne})}{\epsilon/k(\text{Ar})} \quad (5)$$

TABLE II. Predicted melting curve data for the exponential-six potential with $\alpha = 13.2$.

T (K)	p (kbar)	V_s (cm ³ /mol)	V_l (cm ³ /mol)	$\Delta S/R$
24.55	-0.23	14.770	17.709	2.060
60.0	2.87	12.599	13.608	1.330
100.0	7.97	11.176	11.863	1.190
200.0	25.51	9.286	9.731	1.089
300.0	48.17	8.240	8.592	1.053
400.0	75.06	7.530	7.827	1.032
600.0	139.7	6.578	6.813	1.010
800.0	217.2	5.941	6.139	0.997
1000.0	306.6	5.469	5.642	0.988
1500.0	578.0	4.660	4.793	0.971
2000.0	914.0	4.126	4.235	0.960
2500.0	1312.0	3.735	3.827	0.951
3000.0	1772.0	3.430	3.509	0.943

TABLE III. Predicted melting curve data for the exponential-six potential with $\alpha = 14.66$.

$T(\text{K})$	$p(\text{kbar})$	$V_s(\text{cm}^3/\text{mol})$	$V_l(\text{cm}^3/\text{mol})$	$\Delta S/R$
24.55	0.041	13.90	16.40	2.010
60.0	3.34	12.036	13.032	1.371
100.0	8.49	10.806	11.504	1.219
200.0	25.44	9.174	9.656	1.117
300.0	46.51	8.265	8.657	1.078

The scaled Ar and He melting curves are compared with the Ne data in Fig. 5. The scaled Ar experimental and theoretical melting data coincide with the Ne data, showing that these two elements accurately obey a corresponding states relationship, at least over the range 0–60 kbar. The He melting data of Vos *et al.*⁶ fall only slightly below the Ne and Ar data.

The close agreement between the experimental He and theoretical Ar curves in Fig. 5 suggests that the predicted Ar melting curve is indeed accurate even at very high pressures and temperatures. This is consistent with the fitting of the Ar potential to high-pressure solid data to 800 kbar and high-temperature liquid shock-wave measurements to 12 000 K.⁵

IV. CONCLUSIONS

The quasi-isochoric scanning method was successful in measuring the Ne melting curve up to 54.5 kbar. The new high-pressure data smoothly join the older data and a SG fit is found to be a good representation of the melting curve. The high-pressure data now available for He, Ne, and Ar provide a useful data set for testing melting theories and the

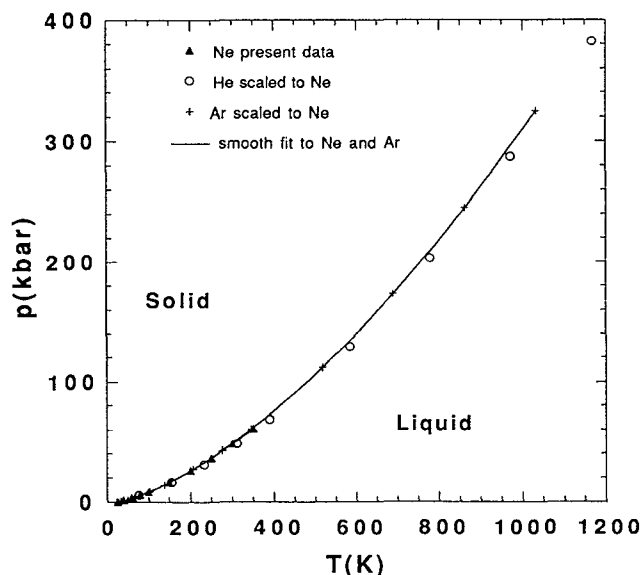


FIG. 5. Neon melting data compared with scaled helium and argon data.

corresponding-states principle.

The present theoretical results show that given an accurate representation of the rare-gas intermolecular potentials, the models of the solid and liquid phases used here are capable of predicting accurately the melting curves. The corresponding-states results suggest further that the melting-curve calculations may be extended to very high pressures and temperatures with confidence.

Over the past decade, there has been considerable interest in the density functional theory (DFT) of melting. While this theory is intellectually appealing and has been applied successfully to the hard-sphere system, the application to real systems has been disappointing.¹⁷ The present method of equating free energies accurately determined by well-established solid and liquid models is more reliable and much easier to use than the rigorous DFT with the necessary third-order corrections.

ACKNOWLEDGMENTS

We thank Peter Kortbeek for useful discussions. WLW acknowledges a Shell "Studiereis" travel fellowship that allowed him to visit LLNL. The work of DAY and MR was performed under the auspices of the U.S. Department of Energy by Lawrence Livermore National Laboratory under contract No. W-7405-Eng-48.

- P. Loubeyre, in *Simple Molecular Systems at Very High Density*, edited by A. Polian, P. Loubeyre, and N. Boccaro (Plenum, New York, 1988), p. 181.
- D. A. Young, C.-S. Zha, R. Boehler, J. Yen, M. Nicol, A. S. Zinn, D. Schiferl, S. Kinkead, R. C. Hanson, and D. A. Pinnick, *Phys. Rev. B* **35**, 5353 (1987).
- D. A. Young and M. Ross, *J. Chem. Phys.* **74**, 6950 (1981).
- D. A. Young, A. K. McMahan, and M. Ross, *Phys. Rev. B* **24**, 5119 (1981).
- C.-S. Zha, R. Boehler, D. A. Young, and M. Ross, *J. Chem. Phys.* **85**, 1034 (1986).
- W. L. Vos, M. G. E. van Hinsberg, and J. A. Schouten, *Phys. Rev. B* **42**, 6106 (1990).
- R. K. Crawford and W. B. Daniels, *J. Chem. Phys.* **55**, 5651 (1971).
- L. W. Finger, R. M. Hazen, G. Zou, H. K. Mao, and P. M. Bell, *Appl. Phys. Lett.* **39**, 892 (1981).
- J. A. Schouten, L. C. van den Bergh, and N. J. Trappeniers, *Rev. Sci. Instrum.* **54**, 1209 (1983).
- G. J. Piermarini, S. Block, J. D. Barnett, and R. A. Forman, *J. Appl. Phys.* **46**, 2774 (1975).
- H. Wieldraaijer, J. A. Schouten, and N. J. Trappeniers, *High Temp. - High Press.* **15**, 87 (1983).
- C. A. Swenson, in *Rare Gas Solids*, edited by M. L. Klein and J. A. Venables (Academic, London, 1977), Chap. 13.
- R. J. Hemley, C.-S. Zha, A. P. Jephcoat, H. K. Mao, L. W. Finger, and D. E. Cox, *Phys. Rev. B* **39**, 11820 (1989).
- P. J. Kortbeek, S. N. Biswas, and J. A. Schouten, *Int. J. Thermophys.* **9**, 803 (1988).
- P. J. Kortbeek and J. A. Schouten, *Mol. Phys.* **69**, 981 (1990).
- R. K. Crawford, in *Rare Gas Solids*, edited by M. L. Klein and J. A. Venables (Academic, London, 1977) Chap. 11.
- A. de Kijper, W. L. Vos, J.-L. Barrat, J.-P. Hansen, and J. A. Schouten, *J. Chem. Phys.* **93**, 5187 (1990).